Journal of Quantitative Spectroscopy & Radiative Transfer 133 (2014) 177–189

Contents lists available at ScienceDirect

Journal of Quantitative Spectroscopy & Radiative Transfer

journal homepage: www.elsevier.com/locate/jqsrt

Simulating polarized light scattering in terrestrial snow based on bicontinuous random medium and Monte Carlo ray tracing

Chuan Xiong [a,b], Jiancheng Shi [a,*]

[a] State Key Laboratory of Remote Sensing Science, Jointly Sponsored by the Institute of Remote Sensing and Digital Earth of Chinese Academy of Sciences and Beijing Normal University, Beijing, China
[b] University of Chinese Academy of Sciences, Beijing, China

ARTICLE INFO

Article history:
Received 27 March 2013
Received in revised form
30 July 2013
Accepted 31 July 2013
Available online 6 August 2013

Keywords:
bicontinuous medium
BRDF
Polarization
Snow
Microstructure

ABSTRACT

To date, the light scattering models of snow consider very little about the real snow microstructures. The ideal spherical or other single shaped particle assumptions in previous snow light scattering models can cause error in light scattering modeling of snow and further cause errors in remote sensing inversion algorithms. This paper tries to build up a snow polarized reflectance model based on bicontinuous medium, with which the real snow microstructure is considered. The accurate specific surface area of bicontinuous medium can be analytically derived. The polarized Monte Carlo ray tracing technique is applied to the computer generated bicontinuous medium. With proper algorithms, the snow surface albedo, bidirectional reflectance distribution function (BRDF) and polarized BRDF can be simulated. The validation of model predicted spectral albedo and bidirectional reflectance factor (BRF) using experiment data shows good results. The relationship between snow surface albedo and snow specific surface area (SSA) were predicted, and this relationship can be used for future improvement of snow specific surface area (SSA) inversion algorithms. The model predicted polarized reflectance is validated and proved accurate, which can be further applied in polarized remote sensing.

1. Introduction

Snow cover is an important part on earth surface. Its high albedo property greatly affects the earth energy budget. Knowledge of snow cover albedo and its temporal variability are important for climatologic and hydrological studies. Thus the simulation and analysis of snow albedo is essential. Also, for remote sensing of snow, forward simulation of snow bidirectional reflectance should be accurate. The inversion of grain size or other parameters from remote sensing data (or field optical and infrared reflectance measurements) requires accurate and robust forward reflectance simulations and comprehensive understanding of light scattering mechanism. By coupling snow parameters development model with snow reflectance model, the snow surface reflectance can be simulated and predicted for climate studies.

The modeling of medium microstructure is important for light scattering simulation. The previous snow reflectance models have different assumptions on snow microstructure. The most often used assumption is sphere based microstructure, with which Mie scattering theory can be applied [42,40]. In this case, the single scattering properties from Mie scattering theory and radiative transfer model can be combined to model snow reflectance. Radiative transfer equations can be solved by various methods, such as discrete ordinates method (such as the DISORT code, [36]), the adding-doubling method [20,34] and spherical-harmonic methods [26,37]. Nolin and Liang [29] made a review of these studies. Nonspherical particle (such as hexagonal particles) was also used to model the single scattering properties of snow, the single scattering properties are calculated by ray tracing [22] and then the single scattering properties are coupled with

* Corresponding author. Tel.: +86 10 64838048.
E-mail address: jshi@irsa.ac.cn (J. Shi).

0022-4073/$ - see front matter © 2013 Elsevier Ltd. All rights reserved.
http://dx.doi.org/10.1016/j.jqsrt.2013.07.026

radiative transfer theory to calculate the reflectance [21,43]. Kokhanovsky and Zege [19] established a simple analytical solution for the radiative transfer equation. Sphere and fractal grains made of multi-size tetrahedrons phase functions were used to simulate the snow surface reflectance.

In some studies, the snow reflectance is directly calculated by ray tracing of snow medium simulated by various methods, or measured from experiment by tomography. Picard et al. [33] modeled the snow medium by single shaped crystals (cubes, cylinders, spheres and sticky spheres). They showed that snow albedo was highly dependent on snow crystal shape. By using different crystal shapes, the albedo–SSA relationship showed very different results. In the model of Kokhanovsky and Zege [19], a shape parameter should be chosen to parameterize the shape of ice particles. Bänninger et al. [2] modeled the snow surface reflectance by ray tracing the measured 2D snow section image. Kaempfer et al. [18] developed a model to simulate the snow medium by a discrete element model or by an X-ray micro-tomography image of snowpack. The three dimensional microstructure of snow was considered in light scattering of snow in Kaempfer et al. [18], but the geometric quantities of the simulated microstructure were uncertain and unknown, so that it cannot be applied to snow parameter inversion algorithms. Also, polarization was not considered in their model. Also, Haussener et al. [16] simulated the macroscopic optical properties of snow based on exact snow morphology image and direct pore-level heat transfer modeling.

The question is which is the proper grain shape for light scattering modeling of snow? In this paper, we try to build a snow reflectance model to solve this problem by using a kind of medium which has good resemblances with real snow microstructure—the bicontinuous medium. The bicontinuous medium can be well controlled and simulated and resembles the real snowpack microstructure. Besides the random non-spherical feature, the size distribution of ice particle is also considered in bicontinuous medium. Further more, this model can take the packing density of the scatterers in the simulated bicontinuous medium into account.

Ding et al. [11] modeled the microwave scattering of bicontinuous random medium by using DDA (discrete dipole approximation), the microstructure simulated by bicontinuous model greatly improved the understanding of microwave remote sensing response to snow, especially for the accurate simulation of cross-polarization signal and frequency behavior of snow microwave scattering. We extend this study into optical and infrared spectrum in this paper. Considering that the wavelength of optical and infrared band is much shorter than the terrestrial snow dimension, the discrete dipole approximation (DDA) cannot be adopted here because of huge computation resource needed. Thus we adopted the Monte Carlo ray tracing technique here to model the light scattering in bicontinuous medium. The albedo, BRDF and polarized BRDF can be simulated by this model.

The generation of bicontinuous microstructure for snow study is discussed first, and then the geometry properties of bicontinuous structure such as specific surface area and equivalent grain size are studied. Then the Monte Carlo ray tracing is applied to the generated microstructure to model BRDF and polarized BRDF as well as albedo of snow surface. Lastly, validation, analysis and discussion of simulation results are presented.

2. Snow 3D microstructure

An important aspect of the light scattering is the simulation and construction of scattering medium microstructure. The microstructure of snowpack is important for the interaction of incident light and snowpack. For optical and infrared light scattering, the penetration depth is usually shallow, thus the microstructure of this shallow layer of snow is responsible for the light scattering of snow covered terrain, and critical for light scattering modeling. Snow forms in the atmosphere by cloud-droplet freezing induced by freezing nuclei and subsequent deposition of water vapor. Depending on the degree of water vapor supersaturation and temperature snow crystals of different shape and size develop. The most prominent of these shapes are stellar dendrites, which resemble stars with a hexagonal symmetry [13]. However, after sintering or other processes on the ground, snow grains are bonded together with each other. Once the snow accumulates on the ground or on top of an already present snowpack the snowpack densifies due to gravity, called settlement, originally separated snowflakes sinter and the original shapes of the snowflakes change according to the present environmental conditions [13]. Then the snow microstructure become very complex and random, which can be verified by microscopy images and section images of terrestrial snow.

In previous models, snow is modeled as a collection of ice particles consisting of only one specific ideal geometric grain shape like spheres, cubes or cylinders. Because of the randomness of terrain snow microstructure, obviously only the spheres, cylinders or other simple and uniform shaped particles cannot represent the real snow morphology. Recently, there were studies which focus on the real microstructure of snow. Kaempfer et al. [18] used the X-ray tomographic snow data and a discrete element model for the snow structure of light scattering simulation and obtained some simulation results. Then they simulated the hemisphere albedo and bidirectional reflectance with ray tracing technique. Bänninger et al. [2] modeled the snow surface reflectance by ray tracing the measured 2D snow section image. However, in order to study the light scattering characteristics of snow with various parameters (density, grain size, and size distribution), snow microstructures data with different parameters should be available. The X-ray tomographic image and 2D snow section image are expensive and not easy to obtain, and the geometric quantities of the discrete element model is uncertain and unknown. We simulated the snow microstructure by the bicontinuous medium we used for microwave snow scattering simulation in this paper. The simulated microstructure keeps largest similarity to the real snow microstructure, and the grain size, density and grain size distribution can be easily controlled.

3. Computer generation of bicontinuous medium

In this paper, we will use the bicontinuous medium to simulate the terrestrial snow. The bicontinuous medium is

a kind of random medium. The basic idea of constructing bicontinuous medium is to generate a kind of medium based on Gaussian random field. A threshold is then used to separate the two phase of medium of Gaussian random field. We outline the general steps for bicontinuous structure generation here.

First, the random field $S(r)$ is generated by Monte Carlo superposition [11]:

$$S(\vec{r}) = \frac{\sum_{n=1}^{N} \cos(\vec{\zeta_n} \cdot \vec{r} + \psi_n)}{\sqrt{N}} \quad (1)$$

In Eq. (1), N is the Monte Carlo superposition number, which should be large enough, for example, $N=10^3$. The wave vector is $\vec{\zeta_n} = \zeta_n \hat{\zeta_n}$. The phase term ψ_n is uniformly random between 0 and 2π. The unit vector $\hat{\zeta_n}$ is uniformly distributed on a unit spherical surface. The wavenumber ζ_n is related to the particle size and particle size distribution in the generated medium. Physically, single size particle is not realistic for snow because there should be a dispersion in snow particle size, thus we should assume a size distribution for the wavenumber ζ_n. According to Chen and Chang [7], the correlation function of the random field generated by (1) can be analytically expressed if we assume wavenumber ζ_n with gamma distribution, and this also gives us convenience to determine the equivalent grain size of bicontinuous medium which is described later on. Moreover, this distribution has previously been found to be a good representation for snow, because particle size with log-normal distribution is suggested for snow according to snow measurements [8], and the gamma distribution is similar to the log-normal distribution. So we follow Ding et al. [11] and Chen and Chang [7] to assume that the wavenumber ζ_n are distributed between 0 and ∞ and follow a gamma distribution probability density function $p(\varsigma)$:

$$p(\varsigma) = \frac{1}{\Gamma(b+1)} \frac{(b+1)^{b+1}}{\langle\varsigma\rangle} \left(\frac{\varsigma}{\langle\varsigma\rangle}\right)^{b} e^{-(b+1)\frac{\varsigma}{\langle\varsigma\rangle}} \quad (2)$$

Γ is the gamma function. $\langle\varsigma\rangle$ is the mean wavenumber which controls the particle size; b is related to the standard deviation of ζ and controls the size distribution.

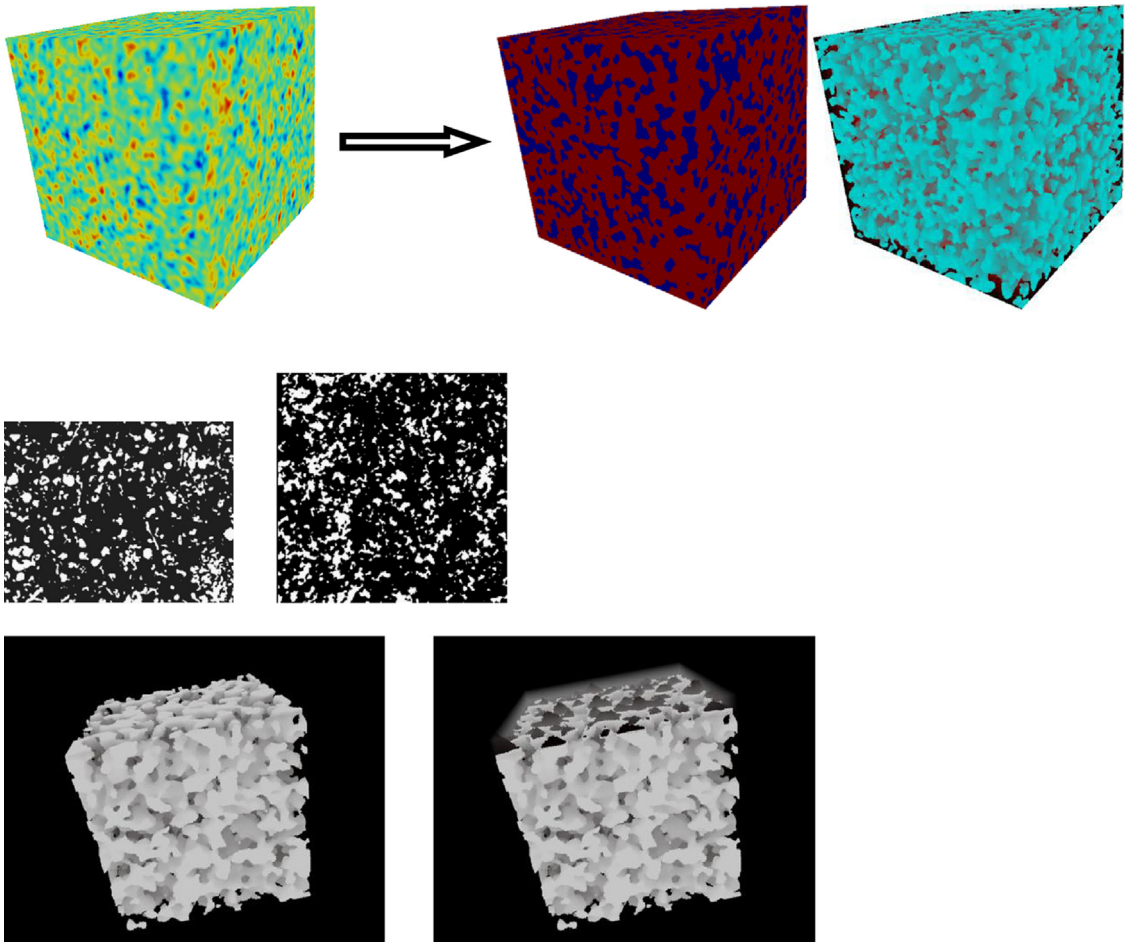

Fig. 1. (upper) Computer generation of bicontinuous medium for snow microstructure simulation, from Gaussian random field to bicontinuous random medium. The $\langle\zeta\rangle$ parameter is 12866.7, the b parameter is 5, and the snow density is 0.27 g/cm^3. The equivalent grain radius is 0.2 mm. The side-length of the cube is 7.5 mm. (middle) left: real snow microstructure shown by section image. right: section image of computer generated bicontinuous medium, with $\langle\zeta\rangle$ parameter 5349.7 and b parameter 1.345, ice phase volume fraction is 0.194. (lower) Particle scale surface roughness added to the cubic simulated bicontinuous medium. Left: Before roughness added, this bicontinuous medium was simulated with equivalent sphere radius 0.1 mm, b parameter 5, and snow density 0.3 g/cm^3; Right: After roughness added, the black pixels indicate the added "cap" to the bicontinuous medium.

Now the random field $S(r)$ is constructed. This field should be cut into two phase which represent ice phase and air phase respectively. The level-cut is performed by

$$\Theta(S(\vec{r})) = \begin{cases} \text{ice}, & \text{when } S(\vec{r}) > \chi \\ \text{air}, & \text{when } S(\vec{r}) \le \chi \end{cases} \tag{3}$$

the χ parameter is determined from the snow density by the following equation

$$\chi = \text{erf}^{-1}(1-2f_v) \tag{4}$$

in conclusion, the bicontinuous structure is constructed by three parameters $\langle\varsigma\rangle$, b and f_v, which control the particle size, particle size distribution and volume fraction respectively. There are good resemblances between the simulated microstructure and real snow microstructure. The bicontinuous medium generation process and the comparison of real snow section image are shown in Fig. 1. We can see from Fig. 1 that the bicontinuous medium is very similar to the snow section image.

A cubic volume of bicontinuous medium is first generated using the method described above. Because the boundary of the generated cubic volume is flat, that is to say, some ice grains near the boundary are cut to flat by the boundary of the cubic volume boundary, and this is not realistic. We avoid this by adding a "cap" to the cubic volume, this simple method is described here. For every ice pixel which is cut by the boundary (on the boundary plane of the cubic volume), certain number of ice pixel is pilled up on this ice pixel. The number of pixels pilled is determined by "minimum number of pixels from this ice pixel to air pixel". The bicontinuous medium before and after this procedure is shown in Fig. 1.

4. Quantitatively determination of the specific surface area (SSA) and equivalent grain radius of bicontinuous medium

The surface area of the simulated microstructure can be derived analytically. Considering a sample bicontinuous medium simulated, if we introduce a phase function $\phi(\vec{r})$ which equals 1 or 0 as the position vector $\vec{r}$ is in ice or air phase respectively. The volume fraction of ice in snow is $f_v = \langle\phi\rangle$. The Debye correlation function which describes the two point correlation of the random bicontinuous medium is defined as

$$p(\vec{r}) = \frac{\langle\phi(\vec{r}_1)\phi(\vec{r}_2)\rangle - {f_v}^2}{f_v(1-f_v)} \tag{5}$$

The correlation length is defined as the derivative of the correlation function at $x=0$:

$$L_c = -\left(\frac{dp(x)}{dx}\right)^{-1}\Big|_{x=0} \tag{6}$$

For bicontinuous medium simulated by gamma distributed ζ, the Debye correlation length of the microstructure can be expressed as (after [4]):

$$L_c = \frac{2\pi\sqrt{3}f_v(1-f_v)}{\langle\varsigma\rangle e^{-(\text{erf}^{-1}(1-2f_v))^2}}\sqrt{\frac{b+1}{b+2}} \tag{7}$$

$\langle\varsigma\rangle, b, f_v$ are the input parameters for bicontinuous microstructure generation.

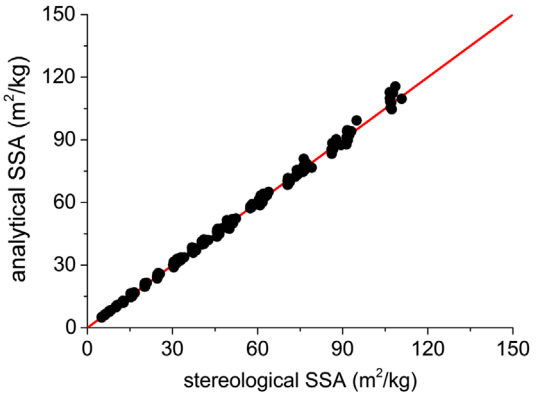

Fig. 2. Validation of analytical SSA expression of bicontinuous medium by stereology. The line is 1:1 line.

According to Debye et al. [10], the Debye correlation length is related to specific surface area (SSA) as

$$SSA = \frac{4f_v(1-f_v)}{\rho_{\text{snow}}L_c} = \frac{4(1-f_v)}{0.918L_c} \tag{8}$$

the SSA here is defined as the ice surface area per unit mass of snow. ρ_{snow} is the density of snow. Based on Eqs. (7) and (8), the SSA of bicontinuous medium can be expressed by the input parameters of medium generation.

On the other hand, the surface area can be estimated by the technique of stereology. To validate the above theory in predicting the SSA of bicontinuous medium, the stereological method was used to calculate the exact surface-to-volume ratio of simulated structure [35]. Direct calculation of surface area from simulated digital image will lead to exaggeration of surface area due to the jagged effect. The basic idea of stereology is to transform a surface area estimation problem to a problem of intersection points counting. A series of bicontinuous microstructures were simulated, then the SSA were calculated based on Eq. (8) and stereology respectively. The results are shown in Fig. 2. They agree very well, which shows that the SSA of bicontinuous medium can be accurately calculated from input parameters.

Furthermore, the size distribution of the bicontinuous medium can be easily controlled by the b parameter. Thus different snow microstructures can be accurately simulated by the bicontinuous medium. In order to maintain equal surface-to-volume ratio compared with spheres, the equivalent sphere radius of bicontinuous medium can be derived as

$$R_e = \frac{3}{0.918SSA} = \frac{3\pi\sqrt{3}f_v}{2\langle\varsigma\rangle e^{-(\text{erf}^{-1}(1-2f_v))^2}}\sqrt{\frac{b+1}{b+2}} \tag{9}$$

5. 3D ray tracing application to bicontinuous random medium

The snow grain radius is normally in the range of 0.05–1.5 mm, which is very large compared to visible and near infrared wavelengths. Then we consider the ray tracing technique could be suitable for the modeling of light scattering in bicontinuous random medium. According to optical

theory, the extinction efficiency for a particle is 2. This is because half of the extinction is due to diffraction; another half is due to geometric optics theory. The diffraction pattern focuses in forward direction with small angular width if the particle dimension is much larger than the wavelength. So the diffracted field can be considered as transmitted field which focuses in forward direction, in this way, the extinction efficiency of a particle can be reduced to 1. Based on this consideration, we then only consider the geometric optics effects take place when light intercepted by a particle in terrestrial snow. Also, neglecting the interference effects, such as the weak localization effect which is the phenomenon of enhanced backscattering from a random medium due to interference effects which occur over distances much larger than the mean free path, is expected to introduce small errors for the snowpack medium considered in this paper. So in this paper we neglect the diffraction effect and the interference effects of light, and only the reflection, refraction and absorption effect are considered.

The basic procedure of ray tracing is: Fire a large number of "photon packs" toward the simulated microstructure; Track the individual "photon" until it goes out of boundary or be absorbed; Gather the "photon packs" in the hemisphere of simulated bicontinuous medium. The firing of "photons" can be assumed as the incident energy towards the snow surface. By nature, the "photon" tracing method is a Monte Carlo method by statistics of the "photon packs" number. Thus a large number of "photons" should be fired in order to obtain precise simulation of reflectance, depending on the wavelength of incident light. The propagation direction of "photons" can be used to simulate the light incident angle. For the case of direct illumination of sunlight without the consideration of diffuse illumination, one fixed propagation direction is used. The diffuse illumination can be simulated by incident "photons" with random incident directions in the hemisphere. It should be noted that the term "photon" we used in this paper is not the same meaning as the photon in quantum electrodynamics, and it is just a representation of Monte-Carlo units of energy. The real quantum electrodynamics photons are actually not localized particles of light [27,28].

Once the photon packs intercepted by the bicontinuous medium, reflection, refraction and absorption will occur. When a light hits an interface, its energy is split into reflected and transmitted ray with proportions given by the Fresnel reflection and transmission coefficients. In this paper we treat this problem with a photon point of view. Only one of the two rays is traced further [18]. The photons are traced until they go out of the medium or are absorbed.

The tracking of an individual photon pack inside the 3D digital image of bicontinuous medium is implemented by digital image processing algorithms. The propagation of photon inside the 3D image is tracked by the digital differential analyzer line generation algorithm of computer graphics. The photon propagates with a certain direction characterized by the azimuth and zenith angle, then the digital differential analyzer algorithm determines which pixel will be the next pixel the photon reaches. When the photon reaches a pixel which is the air-ice or ice-air boundary, the reflection or refraction will occur. The detection of air-ice or ice-air boundary is implemented by judging the previous and present pixel phase (ice or air). The reflection and refraction calculation require the local incident angle to the boundary interface. The local incident angle is calculated based on the propagation direction of photon pack and the normal direction of the boundary. The propagation direction is always tracked in the whole process, thus we only need the normal direction of the intercepted boundary. In this model, the 3D digital image of bicontinuous medium is generated first, and then the normal direction of the boundary pixels can be calculated from the 3D digital image. The x-, y- and z-derivative of the boundary pixels are first calculated by the image processing filters, then the unit normal vector of the boundary is calculated by

$$\vec{n} = \frac{(x', y', z')}{\sqrt{(x')^2 + (y')^2 + (z')^2}}$$

x', y', z' are the directional derivatives of x, y and z direction calculated by filtering operation to the boundary pixels.

The local incident angle of photon incident on the boundary pixel can be calculated from the propagation direction and the local normal vector of the boundary. We consider a photon incident on a boundary, the next step is to determine the photon's fate: reflected or refracted. The determination is made by Monte Carlo concept. The probability of reflection and refraction is determined by the Fresnel reflection and refraction coefficient. Then a random number between 0 and 1 is generated to determine the fate of the photon. The new propagation direction is calculated by the reflection or refraction angle and the previous propagation direction. This can be done by simple vector calculations with Fresnel reflection and refraction. Note that when the photons incident on to ice-air interface, the total reflection should be taken into account.

When the photon propagates through the ice phase of the bicontinuous medium, absorption effect occurs. In the same way, we treat this problem with Monte Carlo concept by the probability of absorption. According to Beer's law, the intensity left after light propagating through a path of length L is

$$I' = e^{-\kappa_a L} I$$

I' is the intensity left after propagation, I is the initial intensity, κ_a is the absorption coefficient of ice under certain temperature and frequency condition. The absorption coefficient is given by [5]

$$\kappa_a = \frac{4\pi n_{imag}}{\lambda}$$

n_{imag} is the imaginary part of ice refractive index, λ is the wavelength. The refractive index of ice is calculated according to Warren [41] in this paper.

The proportion of intensity absorbed is

$$\frac{I^{abs}}{I} = \frac{I - I'}{I} = 1 - e^{-\kappa_a L}$$

This means that when a photon propagates through a path in ice of length L, the probability of absorption is

$$P^{abs} = 1 - e^{-\kappa_a L}$$

In the same way as reflection and refraction, a random number between 0 and 1 is generated to compare with the

probability of absorption, if the random number is smaller than the probability of absorption, this photon is absorbed.

Due to the limit of computer memory, limited length of bicontinuous medium cube can be generated for ray tracing. In order to obtain infinite microstructure, the computer generated 3D image of bicontinuous medium is expanded in x, y and z direction. Conceptually, the edge of computer generated bicontinuous microstructure is like a mirror and the pixels out of the edge are mirrored into the pixels inside the edge to determine if it is in ice or air phase.

The reflectance of the snow medium is calculated by the photons escaping out of the snow medium into the hemisphere. The photon number is counted in each direction. In order to simulate the bidirectional reflectance, the hemisphere above the snow medium is divided into small patches and the photons are collected in each small patch. The dividing of the hemisphere is important. If the patches are divided with equal zenith and azimuth angle, the patches near the pole will have very large solid angle. In this paper, we follow Parviainen and Muinonen [30] to divide the hemisphere. First the hemisphere is evenly divided in the zenith angle direction so that the zenith angle is divided into n_θ parts. Then in each zenith angle area, the azimuth angle is evenly divided into n_ϕ parts so that the mean solid angle of a single patch is close to the solid angle of the pole patch, with zenith angle width of $\Delta\theta$ and azimuth angle width of 2π

$$\Omega_0 = \int_0^{2\pi} d\phi \int_0^{\Delta\theta} \sin(\theta)\, d\theta = 2\pi(1-\cos(\Delta\theta))$$

θ is the zenith angle, ϕ is the azimuth angle.

Then the photons can be collected in patches in the hemisphere with nearly equal solid angles.

The bidirectional reflectance factor (BRF) and albedo of snow scene can be simulated by ray tracing. Albedo is defined by the ratio of energy reflected into the hemisphere and the energy incident to the scene. Obviously, the albedo can be simply determined by the number of photons escape out to the hemisphere and the total number of photons fired:

$$albedo = \frac{N_{hemi}}{N_{total}}$$

The bidirectional reflectance distribution function (BRDF) quantifies the radiance scattered into all directions from a surface illuminated by a source from any direction above the hemisphere of the material. The BRDF is given by

$$BRDF = \frac{dL(\theta,\phi)}{dE(\theta',\phi')}$$

$dL(\theta,\phi)$ is the reflected received, $dE(\theta',\phi')$ is the incident flux density (irradiance).

The received radiance can be expressed by:

$$dL(\theta,\phi) = \frac{d^2\Phi_{ref}}{d\Omega\, d(A\cos\theta_{ref})}$$

$d^2\Phi_{ref}$ is the reflected flux, $d\Omega$ is the solid angle of the divided element patch on the hemisphere, dA is the surface area on the snow surface, θ_{ref} is the zenith angle of the receiving patch on the hemisphere.

The incident flux density can be expressed by

$$dE(\theta',\phi') = \frac{d\Phi_{inc}}{dA}$$

$d\Phi_{inc}$ is the incident flux.

Then the BRDF can be derived as

$$BRDF = \frac{d^2\Phi_{ref}}{d\Phi_{inc}} \frac{1}{\cos\theta_{ref}\, d\Omega} = \frac{n_{ref}}{n_{inc}\cos\theta_{ref}\, d\Omega}$$

n_{ref} is the number of photons received, n_{inc} is the number of photons fired onto the bicontinuous medium surface.

The bidirectional reflectance factor can be expressed by

$$BRF = \pi\, BRDF = \frac{\pi n_{ref}}{n_{inc}\cos\theta_{ref}\, d\Omega}$$

Finally, by collecting and count the photons on the patches on the hemisphere, the BRF and BRDF can be simulated.

In this model, the polarimetric BRDF of snow is also simulated. The method to account for the polarized signature of light reflected by the snow surface is presented here. Detailed description of the scattering of light typically express the light as the Stokes vector $\vec{S} = (I, Q, U, V)$, where I, Q, U, V have been defined by Van de Hulst [39]. The I parameter represents the intensity of light, and Q, U, V describe the polarization state of light. In order to include the 4 Stokes parameters during the ray tracing process, polarimetric Fresnel reflection and refraction are used for the reflection and refraction calculations.

$$S' = \begin{bmatrix} I' \\ Q' \\ U' \\ V' \end{bmatrix} = M \bullet S = \begin{pmatrix} m_{00} & m_{01} & m_{02} & m_{03} \\ m_{10} & m_{11} & m_{12} & m_{13} \\ m_{20} & m_{21} & m_{22} & m_{23} \\ m_{30} & m_{31} & m_{32} & m_{33} \end{pmatrix} \begin{bmatrix} I \\ Q \\ U \\ V \end{bmatrix}$$

In the above equation, the M matrix is the flat surface Fresnel's reflection and refraction matrix for polarized reflection and transmission.

For polarimetric case, the polarization signature of photons should be traced. The Fresnel reflection and refraction matrix are based on the so called 1–2 polarization system [38], the perpendicular polarization direction is perpendicular to both incident direction and scattering direction, and the parallel polarization is perpendicular to both perpendicular polarization direction and propagation direction. The polarization reference frame changes during the photon scattering process, so the polarization reference frame should be recalculated each time when reflection or transmission takes places. The polarization reference frame change is shown in Fig. 3.

The incident light Stokes vector is first rotated from the polarization reference frame of previous reflection or refraction process (*PD1* to *PD2*) to the new polarization reference frame of present reflection or refraction process (*PD2* to *PD3*), then multiplied by the Fresnel reflection or refraction matrix

$$S' = M \bullet K \bullet S$$

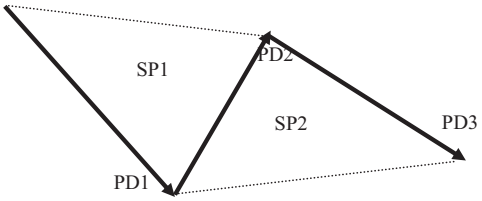

Fig. 3. Photon propagation and polarization direction tracing. Propagation direction 1 (PD1), Propagation direction 2 (PD2) and Propagation direction 3 (PD3) are three photon propagation directions. In scattering process from PD1 to PD2, the perpendicular polarization direction of PD2 is perpendicular to scattering plane 1 (SP1), which is defined by PD1 and PD2; in the scattering process from PD2 to PD3, the perpendicular polarization direction of PD2 is perpendicular to scattering plane 2 (SP2), which is defined by PD2 and PD3. The polarization reference frame of PD2 is rotated in these two scattering processes to track the polarization state.

K is the rotation matrix of Stokes vector [after [15]]

$$K=\begin{pmatrix}1 & 0 & 0 & 0\\ 0 & \cos(2\omega) & \sin(2\omega) & 0\\ 0 & -\sin(2\omega) & \cos(2\omega) & 0\\ 0 & 0 & 0 & 1\end{pmatrix}$$

ω is the polarization direction rotation angle. From Fig. 3, ω can be calculated by the rotation angle of perpendicular polarization directions. In other words, the perpendicular polarization direction of Propagation Direction 2 (*PD2*) rotated by ω from the polarization reference frame of *PD1* & *PD2* to the polarization reference frame of *PD2* & *PD3*. The perpendicular polarization direction can be calculated by cross product of propagation direction vectors. Finally, after the photon escape out into the hemisphere, the Stokes vector should be multiplied by a rotation matrix K again to convert the Stokes vector into the polarization reference frame defined by incident photon direction and sensor viewing direction (the propagation direction of escaped photon).

We assume the incident sunlight is unpolarized so that the Stokes parameter of incident light is

$$S_{inc}=\begin{bmatrix}1\\0\\0\\0\end{bmatrix}$$

In polarized case, the BRDF is calculated by

$$BRDF=\frac{dI(\theta,\phi)}{dE(\theta',\phi')}$$

I is the first element of Stokes parameters.

The polarized BRDF is expressed by

$$BRDF_{pol}=\frac{\sqrt{dQ^2(\theta,\phi)+dU^2(\theta,\phi)+dV^2(\theta,\phi)}}{dE(\theta',\phi')}$$

In this model, the photon number is used to simulate the intensity of light based on Monte Carlo point of view. Thus the I parameter can be simply simulated by the number of photons, and Q,U, V parameter can be simulated by the number of photons and the relative value between I and Q, U, V of each photon. That means when collecting photons, when the number of photon increase 1, if the photon number used to calculate I parameter increases by 1, then the photon number used to calculate Q,U, V parameters increases by $Q_p/I_p, U_p/I_p, V_p/I_p$ respectively, I_p, Q_p, U_p, V_p are the values of Stokes parameters of the individual collected photon.

6. Results and analysis

6.1. Albedo simulation

6.1.1. Spectral albedo

Albedo is the ratio of the upward reflected flux over the incoming direct solar flux. The albedo of snow surface greatly affects the energy balance of earth due to its high value. In many studies, the albedo–SSA relationship was studied and it was used for SSA inversion. Also, by combined with snow SSA evolution model, the albedo–SSA relationship can be used for predicting the evolution of snow albedo, and how this will change in a climate changing world.

First we validated the ray tracing procedure's accuracy by comparing the spectral albedo ray tracing of random non-sticky spheres with Mishchenko model [26] in which Mie theory is used for single scattering calculation (we call it Mishchenko–Mie model hereafter). The random non-sticky spheres medium was constructed by randomly placing spheres in a box, which were then used for ray tracing. We call this model as sphere-PT model, and the ray tracing of bicontinuous medium as bic-PT model hereafter. The result of spectral albedo with sphere radius of 0.05 mm, 0.1 mm and 0.4 mm are shown in Fig. 4a. We can see that the agreement between our result and the Mishchenko–Mie model result is nearly perfect. This conclusion verified the validity of the ray tracing procedure applied in this paper, and shows that the assumption of geometric optics and ray tracing will not cause much error in hemispherical reflectance modeling.

Many models of snow albedo represent snow crystals by spheres of surface/volume (S/V) ratio equal to that of snow crystals, such as the DISORT model and Mishchenko–Mie model. But there is always a doubt about the validity of the representation of snow microstructure by sphere particles. Here we will simulate the snow spectral albedo by ray tracing of both bicontinuous medium and random non-sticky spheres separately. These two kinds of medium have the same SSA and density value. The two models are used to validate the albedo measurement data of Brandt [6]. The result is also shown in Fig. 4b. We can see from the figure that the ray tracing model with bicontinuous medium predicted nearly equal spectral albedo with the ray tracing model with non-sticky spheres under diffuse illumination. The modeled spectral albedo agree well with the measured albedo, the underestimation of wavelengths shorter than 800 nm is caused by the leak of photons due to the limitation of computer resourses and small absorption coefficient.

The models based on classical radiative transfer theory (such as [36,20,26,37,1]) is derived based on low packing density and independent scattering assumption, thus the models based on classical radiative transfer theory are not valid in principle for high packing density medium such as snow. Mishchenko [24] and Mishchenko and Macke [25]

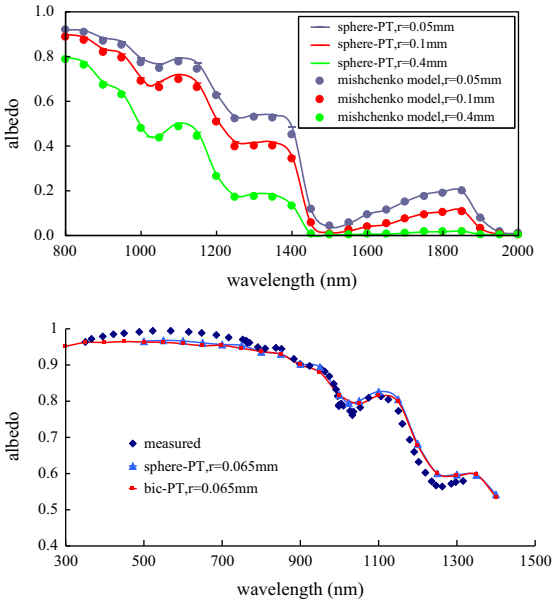

Fig. 4. (upper) Spectral albedo predicted by Mishchenko model and ray tracing of random non-sticky spheres (sphere-PT) with sphere radius of 0.05 mm, 0.1 mm and 0.4 mm and normal incidence. (lower) Spectral albedo measured by Brandt et al. [6] with diffuse incidence and rounded snow grains and its validation using ray tracing of bicontinuous medium (bic-PT) and non-sticky spheres (sphere-PT). The sphere radius is set to be 0.065 mm in both cases.

used a dense medium light scattering theory based on the introduction of the static structure factor to calculate asymmetry parameters of the phase function for densely packed particles. They showed that in geometrical optics limit, the approximation of independent scattering gives reasonably good accuracy and may be used in practical computations for densely packed grains such as snow medium, and the classical radiative transfer equation can give good results for big non-absorbing or moderately absorbing particles, such as ice particles in snow. Dlugach and Mishchenko et al. [9] simulated the light scattering in densely packed random particulate medium by numerically exact method, their simulations showed that in the case of very large values of the particle packing density, the scattering characteristics of the particulate volume start to exhibit behavior not predicted by the low-density theories of coherent backscattering and radiative transfer. Nevertheless, the direct computer solutions of the Maxwell equations do demonstrate that the classical low-density predictions can survive (at least in a qualitative and even semi-quantitative sense) volume packing densities typical of particle suspensions and particulate surfaces encountered in natural and man-made conditions. The dense media effect of electromagnetic scattering is very apparent when wavelength is comparable to scattering particle dimension, for example, the microwave scattering in snow [40], and the numerical simulations of Mackowski and Mishchenko [23]. However, in the case of visible and near-infrared light scattering in snow, the grain sizes and spaces between ice grains are very large compared with the wavelength of light, so the models based on classical radiative transfer theory were practically used for dense media such as snow (such as [42,26,31]). Warren [40] also stated that for snow density smaller than 0.45 g/cm^3, the near-field scattering would be unimportant. The experiment of Bohren and Beschta [44] also indicate that the snow density has very limited effect on the snow albedo. We carried out some simulaitons using our bic-PT model to test the albedo's sensitivity to snow density, an example is shown in Fig. 5. From Fig. 5 we can see that the snow density has very little effect on the albedo. In Fig. 5, we also showed that the grain size distribution parameter *b* has little effect on the snow albedo.

6.1.2. *Albedo–SSA relationship*

Hemispherical reflectance is less affected by the shape of scattering particles than bidirectional reflectance [14], so hemispherical reflectance is recommended to invert the size of scattering particles rather than bidirectional reflectance. For example, Gallet et al. [12] developed a system called “DUFISSS” to measure the hemispherical reflectance of snow sample, then the snow SSA is retrieved according to the measured hemispherical reflectance. For the

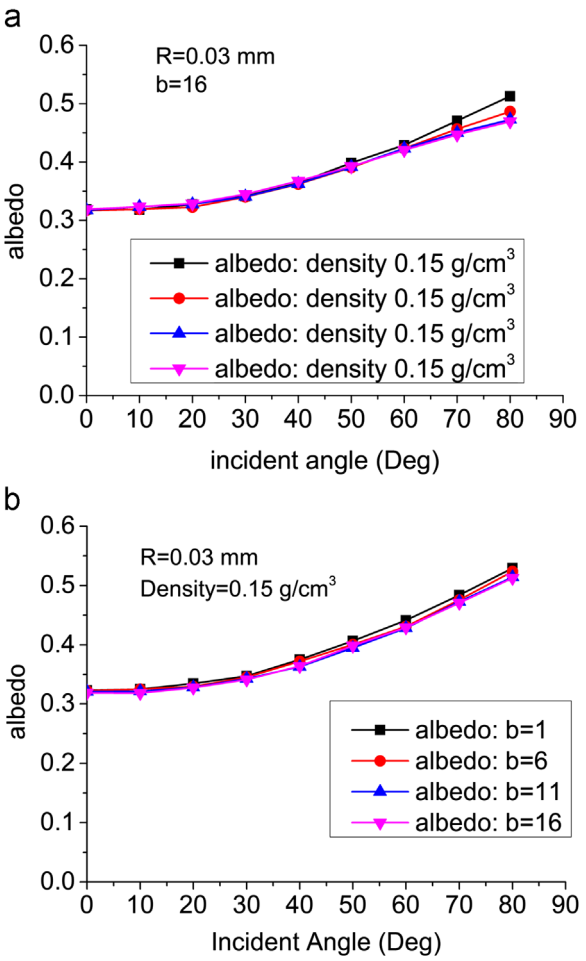

Fig. 5. (upper) Plane albedo sensitivity to snow density simulated by bic-PT model. Equivalent sphere radius is 0.03 mm, *b* parameter is 16, wavelength is 1800 nm. (lower) Plane albedo sensitivity to *b* parameter simulated by bic-PT model. Equivalent sphere radius is 0.03 mm, snow density of 0.15 g/cm^3, wavelength is 1800 nm.

purpose of estimating snow SSA from spectral reflectance measurements, the SSA–albedo relationship of snow is investigated by our model in this section.

Gallet et al. [12] measured the snow albedo–SSA relationship by experiments. The snow albedo was measured by their DUFISSS device with normal incident radiation of laser diodes along with SSA and density measurements. Picard et al. [33] modeled the snow medium by single shaped crystals (cubes, cylinders, spheres and sticky spheres). Then ray tracing technique was then applied to the simulated medium to simulate snow surface albedo. Also, the model of Kokhanovsky and Zege [19] needs *a b* parameter to indicate the crystal shape. Picard et al. [33] showed that the albedo–SSA relationship was highly dependent on the snow crystal shape. Their results showd that the model based on ray tracing technique and snow medium composed of non-sticky spheres predicted almost the same results with DISORT model under normal illumination, wheras the cubes, cylinders, and sticky spheres based ray tracing model predicted higher albedo than non-sticky spheres based model for the same snow SSA value under normal illumination. We investigated the albedo–SSA relationship by using the bicontinuous medium here, which has larger similarity to the real snow crystal shape.

Various snow parameters (snow SSA, density and size distribution parameters) were used for albedo simulations by the bic-PT model and sphere-PT model. The albedo–SSA relationships at 1310 nm and 1550 nm of semi-infinite single layer snow predicted by the two models are shown in Fig. 6. We found from the simulation results that the size distribution parameter b and the snow density have very little effect on the albedo, so Fig. 6 was plotted with equivalent sphere radius from 0.02 mm to 0.6 mm with 0.02 mm step in bic-PT model. The b parameter is fixed to 10, and the volume fraction of ice is fixed to 0.25 g/cm^3. As shown in Fig. 6, the bic-pt model predicted slightly higher albedo than the sphere-PT model under normal incidence and equal albedo with the shere-sphere model under diffuse illumination. The SSA–albedo relationship of bicontinuous medium under normal incident light is similar to the SSA–albedo relationship predicted by medium composed of sticky spheres as reported in Picard et al. [33]. This may be due to the fact that sticky spheres is also similar to the snow microstructure, and this is also the reason for using sticky spheres in modeling microwave scattering in snow [40]. Also,

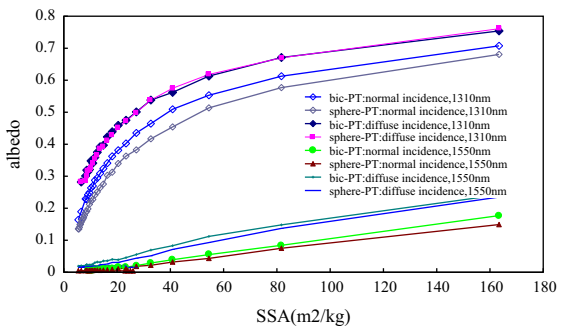

Fig. 6. SSA–albedo relationship predicted by bic-PT model and bic-sphere model under normal incidence and diffuse incidence at wavelength of 1310 nm and 1550 nm.

as mentioned before, by simulating albedo with different snow parameters, we found that the SSA–albedo relationship is very little affected by the snow density and ice particle size distribution.

6.2. Bidirectional reflectance simulations

To test the model performance on directional reflectance, we validated the model with the experiment of Hudson et al. [17]. The measurements were conducted on the Dome C (75°06′S, 123°18′E, 3200 m MSL) of Antarctic. Both the spectral albedo and the BRF of snow surface were measured on a 32 m tower. The measurements were made with the effects of sastrugi with small scale roughness on snow surface.

First, the data presented in Fig. 3 of Hudson et al. [17] is validated. We used an equivalent sphere radius of 0.06 mm for equivalent grain radius, and 10 for grain size distribution parameter *b*. The snow density was set to be 0.27 g/cm^3. Under 52.8° and 69.3° solar incident zenith angle, the 1800 nm BRF and polarized BRF is first simulated. 10,000,000 photons were fired in the simulation. The validation is shown in Fig. 7. The anisotropic reflectance factor (ARF) is defined by

$$R(\theta_s, \phi_s, \theta_i) = \frac{BRF}{A}$$

A is the plane albedo, θ_s is the zenith angle of observation direction, ϕ_s is the relative azimuth angle of observation direction, θ_i is the solar zenith angle.

The albedo predicted by the bic-PT model is 0.2832 and 0.337 for 52.8° and 69.3° incidence respectively. We can see from Fig. 7 that the agreement between bic-PT model simulated and observed anisotropic reflectance factor is good. The simulated anisotropic reflectance factor value of forward and backward observation direction is very close to the observation data, and the trend agree very well. We also simulated the anisotropic reflectance factor by the Mishchenko–Mie model. The input snow grain radius is also 0.06 mm. The albedo predicted by the Mishchenko–Mie model is 0.243 and 0.328 for 52.8° and 69.3° incidence respectively. The simulated anisotropic reflectance factor is also shown in Fig. 7. Obviously, the Mishchenko–Mie model overestimated the reflectance in the forward direction and underestimated the reflectance in the backward direction. There are two possible explanations for this: First, the Mishchenko–Mie model assumes spherical snow grains, but the actual snow grain is not really spherical, thus the Mie theory cannot predict the phase function of snow medium correctely; Secondly, the Mishchenko–Mie model assumes totally flat air–snow interface. The bic-PT model assumes bicontinuous random microstructure, in which the small scale snow surface roughness is considered. We also simulated the bidirectional reflectance measurement with incident angle of 52.8° and 69.3° at 600 nm. The Mishchenko–Mie model and bic-PT model result of 600 nm is shown in Fig. 8. In bic-PT model, an equivalent sphere radius of 0.06 mm was used, and 10 was used for grain size distribution parameter *b*. The snow density was set to be 0.27 g/cm^3. 500,000 photons were fired in the simulation. In Mishchenko–Mie model, the sphere radius was set to be 0.06 mm. The albedo predicted by both model is close to 1.

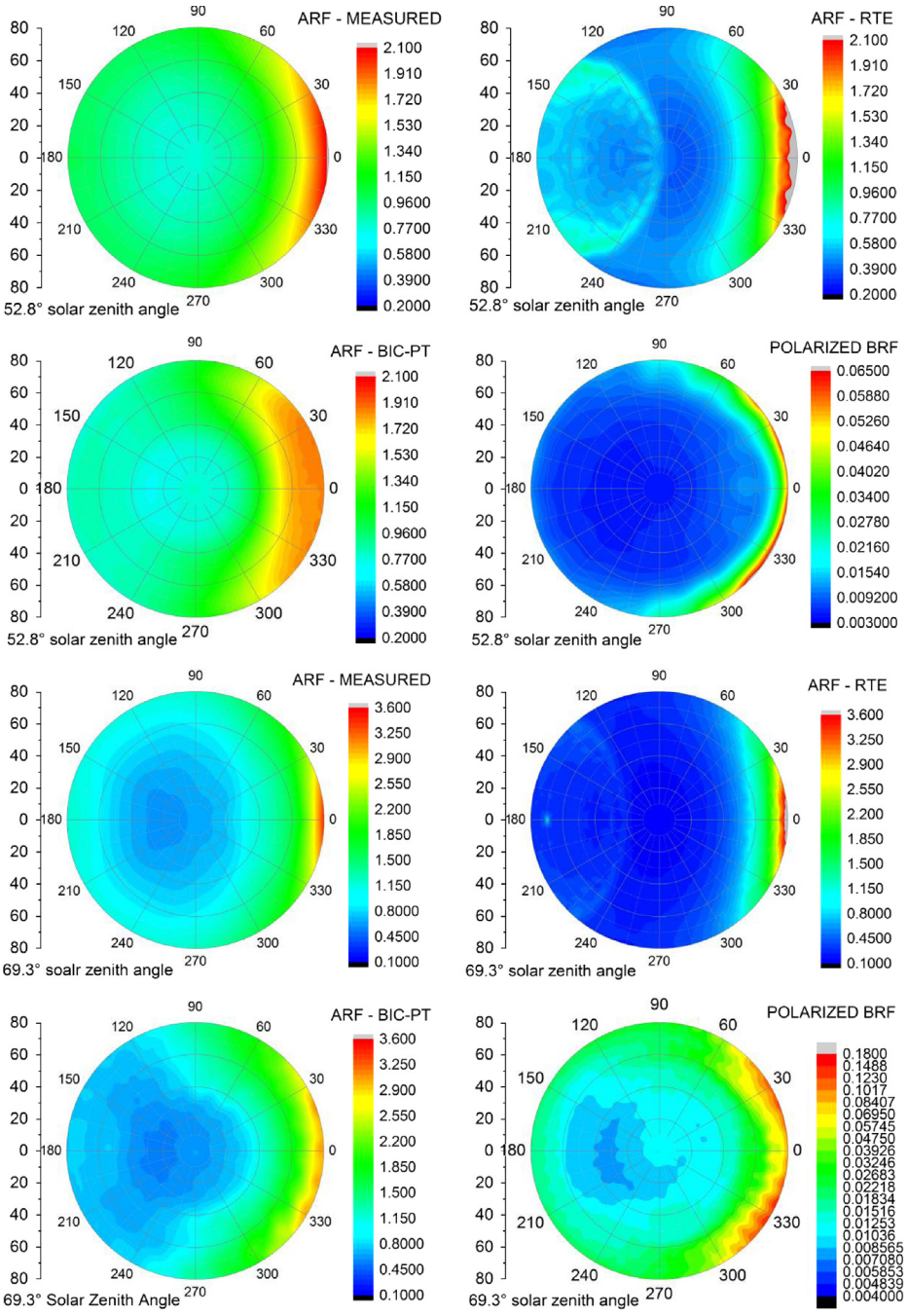

Fig. 7. Validation of bidirectional reflectance measurement with incident angle of 52.8° and 69.3° at 1800 nm. The polarized BRF are also showed. The foward observation direction is on the right.

We can see from the model results that the bic-PT successfully predicted the weak anisotropy feature of the bidirectional reflectance of 52.8° incidence at 600 nm, but the Mishchenko–Mie model overestimated the foward reflectance and underestimated the reflectance at backward direction. Generally, the bic-PT model predicted much better anisotropy pattern than the Mishchenko–Mie model which is based on Mie theory and radiative transfer equation.

The inversion of snow grain size from bidirectional reflectance data was investigated in several studies. Painter et al. [32] and Berisford et al. [3] developed devices to measure the snow grain size by bidirectional reflectance. Their inversion algorithm was based on the Mie and DISORT model, which assumes spherical ice particles in snow. Improvement is expected if our model is applied to the grain size (or SSA) inversion algorithm.

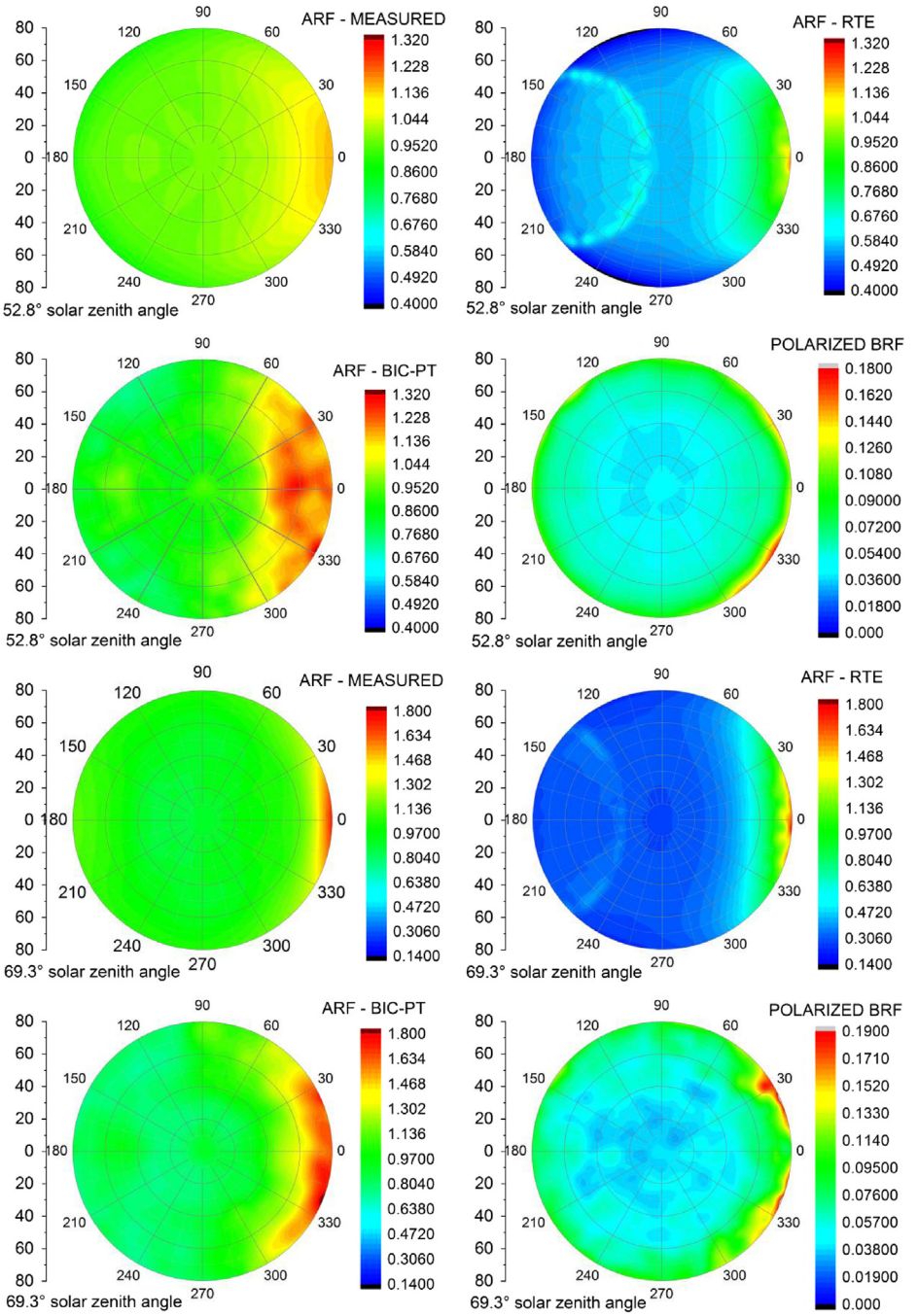

Fig. 8. Validation of bidirectional reflectance measurement with incident angle of 52.8° and 69.3° at 600 nm. The polarized BRF are also showed. The foward observation direction is on the right.

6.3. *Polarized reflectance simulations*

We can see from the polarized BRF shown in Figs. 7 and 8 that the polarized reflectance of snow surface is not negligible. The pattern of polarized BRF is similar to the BRF. The polarization of snow surface should be considered in polarized remote sensing. In order to validate the absolute value of polarized reflectance simulated by the model, we simulated the polarized reflectance in the experiment carried out by Leroux et al. [20]. The wavelength is 1650 nm and the incident solar zenith angle is 62.36°. According to their description, the surface snow layer is composed by clustered rounded ice grains. We simulated with equivalent grain radius of 0.27 mm, grain size distribution parameter of 100, and density of 0.45 kg/m^3. The simulation results is shown in Fig. 9. The reflectance and polarized reflectance in Fig. 9 is

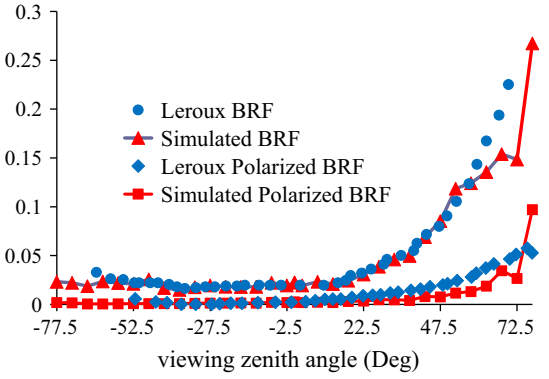

Fig. 9. Simulations of snow surface reflectance and polarized reflectance in the principle plane. Positive zenith angle indicates forward viewing direction and negative zenith angle indicates backward viewing direction.

defined according to the Leroux et al. [20] paper, which are actually BRF and polarized BRF value respectively. We can see from Fig. 9 that our simulated reflectance and polarized reflectance are very close to the experiment data of Leroux et al. [20].

7. Summary and conclusion

In this paper we presented an approach for snow reflectance modeling based on bicontinuous random medium and ray tracing. The spherical or other single shaped particles cannot represent the real snow microstructures. Meanwhile, the bicontinuous medium can simulate the real snow microstructure, without assuming single shaped particles. Grain size, density and grain size distribution can be easily controlled in the bicontinuous medium generation algorithm. According to the bicontinuous medium construction principles, the specific surface area (SSA) of bicontinuous medium can be expressed analytically by the input parameters. This SSA expression is validated by stereology technique and proved very accurate.

Monte Carlo ray tracing is applied to the computer generated bicontinuous medium to simulate the snow reflectance. Due to the large grain size of terrestrial snow compared to the wavelength, the geometric optic theory is a good approximation. The diffraction is assumed to be in forward direction, so only the reflection, refraction and absorption effect is considered. This makes ray tracing technique applicable to terrestrial snow. The Stokes parameters and polarization direction are traced during the ray tracing process, thus both BRF and polarized BRF can be simulated.

With our model, the snow surface albedo, diffuse albedo, BRF and polarized BRF can be simulated. The spectral albedo is validated and the agreement is very good. Simulation results showed that the albedo is not very sensitive to the grain shape, and the sphere based model can be used for efficient snow albedo simulation. The modeled albedo–SSA relationship by the bic-PT model shows that the relationship is similar to the SSA–albedo relationship predicted by sticky spheres under normal incidence light, and it is close to the SSA–albedo relationship predicted by non-sticky spheres.

The BRF simulation is validated with the experimental result of Hudson et al. [17]. The model provides better result compared to Mishchenko–Mie model which uses the Mie theory and radiative transfer equation. Meanwhile, the polarized BRF results were presented and validated. It is important for polarized aerosol remote sensing. The model predicted bidirectional reflectance result can be further applied to snow grain size inversion from bidirectional reflectance measurement.

In this paper, the reflectance model of dry snow surface is constructed. In many area, the snow is wet so that liquid water exists in snow. In addition to two-phase system, we can simulate the three-phase system microstructure using the bicontinuous medium. According to Berk [4], the two-phase system can be simulated by considering $\beta \to +\infty$, which is the special case we described in Section 3 for dry snow simulation. If we calculate β according to the volum fraction of a third phase, the three-phase system can be simulated. Future work should be the investigation of the effect of liquid water on the reflectance of terrestrail snow surface.

Acknowledgments

This work was supported by the CAS/SAFEA International Partnership Program for Creative Research Teams (No. KZZD-EW-TZ-09) and the National Natural Science Foundation of China (41001211). The authors are grateful to the reviewers and an editor for their valuable comments and suggestions.

References

[1] Aoki Te, Aoki Ta, Fukabori M, Hachikubo A, Tachibana Y, Nishio F. Effects of snow physical parameters on spectral albedo and bidirectional reflectance of snow surface. J Geophys Res 2000;105:10219–36.
[2] Bänninger D, Bourgeois CS, Matzl M, Schneebeli M. Reflectance modeling for real snow structures using a beam tracing model. Sensors 2008;8(5):3482–96.
[3] Berisford Daniel F, Molotch Noah P, Durand Michael T, Thomas HPainter. Portable spectral profiler probe for rapid snow grain size stratigraphy. Cold Reg Sci Technol 2013;85:183–90.
[4] Berk NF. Scattering properties of the leveled-wave model of random morphologies. Phys Rev A 1991;44(8):5069.
[5] Born M, Wolf E. Principles of optics. 3rd ed.New York: Pergamon; 808.
[6] Brandt, R. E., Warren, S.G., and Clarke, A.D.: A controlled snowmaking experiment testing the relation between black carbon content and reduction of snow albedo, J Geophys Res,116, D08109, 10.1029/2010JD015330, 2011.
[7] Chen SH, Chang SL. Simulation of bicontinuous microemulsions: comparison of simulated real-space microstructures with scattering experiments. J Appl Crystallogr 1991;24:721–31.
[8] Colbeck SC. Statistics of coarsening in water-saturated snow. Acta Metall 1986;34:347–52.
[9] Dlugach JM, Mishchenko MI, Liu L, Mackowski DW. Numerically exact computer simulations of light scattering by densely packed, random particulate media. J Quant Spectrosc Radiat Transfer 2011;112:2068–78.
[10] Debye PJW, Anderson HR, Brumberger H. Scattering by an inhomogeneous solid II. The correlation function and its application. J Appl Phys 1957;28:679–83.
[11] Ding Kung-Hau, Xu Xiaolan, Leung Tsang. Electromagnetic scattering by bicontinuous random microstructures with discrete permittivities. IEEE Trans Geosci Remote Sens 2010;48(8):3139–51.

[12] Gallet, J.-C., Domine, F., Zender, C.S., and Picard, G.: Measurement of the specific surface area of snow using infrared reflectance in an integrating sphere at 1310 and 1550 nm, Cryosphere, 3, 167-182, 10.5194/tc-3-167-2009, 2009.
[13] Gergely Mathias. Snow characterization by optical properties.Germany: Ruperto-Carola University of Heidelberg; 2011.
[14] Grenfell TC, Warren SG, Mullen PC. Reflection of solar radiation by the Antarctic snow surface at ultraviolet, visible, and near-infrared wavelengths. J Geophys Res 1994;99:18669–84.
[15] Grynko Ye, Shkuratov Yu. Scattering matrix calculated in geometric optics approximation for semitransparent particles faceted with various shapes. J Quant Spectrosc Radiat Transfer 2003;78(3–4):319–40.
[16] Haussener S, Gergely M, Schneebeli M, Steinfeld A. Determination of the macroscopic optical properties of snow based on exact morphology and direct pore-level heat transfer modeling. J Geophys Res 2012;117(F3):F03009. http://dx.doi.org/10.1029/2012JF002332.
[17] Hudson SR, Warren SG, Brandt RE, Grenfell TC, Six D. Spectral bidirectional reflectance of Antarctic snow: measurements and parameterization. J Geophys Res 2006;111:D18106.
[18] Kaempfer TU, Hopkins MA, Perovich DK. A three-dimensional microstructure-based photon-tracking model of radiative transfer in snow. J Geophys Res 2007;112:D24113.
[19] Kokhanovsky Alexander A, Zege Eleonora P. Scattering optics of snow. Appl Opt 2004;43(7):1589–602.
[20] Leroux C, Deuze JL, Goloub P, Sergent C, Fily M. Ground measurements of the polarized bidirectional reflectance of snow in the near-infrared spectral domain: comparisons with model results. J Geophys Res Atmos 1998;103(D16):19721–31.
[21] Leroux C, Lenoble J, Brogniez G, Hovenier JW, De Haan JF. A model for the bidirectional polarized reflectance of snow. J Quant Spectrosc Radiat Transfer 1999;61(3):273–85.
[22] Macke A, Mishchenko MI. Applicability of regular particles shapes in light scattering calculations for atmospheric ice particles. Appl Opt 1996;35:4291–6.
[23] Mackowski DW, Mishchenko MI. Direct simulation of extinction in a slab of spherical particles. J Quant Spectrosc Radiat Transfer 2013;123:103–12.
[24] Mishchenko MI. Asymmetry parameters of the phase function for densely packed scattering grains. J Quant Spectrosc Radiat Transfer 1994;52:95–110. http://dx.doi.org/10.1016/0022-4073(94)90142-2.
[25] Mishchenko MI, Macke A. Asymmetry parameters of the phase function for isolated and densely packed spherical particles with multiple internal inclusions in the geometric optics limit. J Quant Spectrosc Radiat Transfer 1997;57:767–94.
[26] Mishchenko M, Dlugach JM, Yanovitskij EG, Zakharova NT. Bidirectional reflectance of flat, optically thick particulate layers: an efficient radiative transfer solution and applications to snow and soil surfaces. J Quant Spectrosc Radiat Transfer 1999;63:409–32.
[27] Mishchenko MI. Multiple scattering, radiative transfer, and weak localization in discrete random media: unified microphysical approach. Rev Geophys 2008;46:RG2003.
[28] Mishchenko MI. Gustav Mie and the fundamental concept of electromagnetic scattering by particles: a perspective. J Quant Spectrosc Radiat Transfer 2009;110:1210–22.
[29] Nolin A, Liang S. Progress in surface particulate medium bidirectional reflectance modeling and applications. Remote Sens Rev 2000;18:281–306.
[30] Parviainen Hannu, Muinonen Karri. Bidirectional reflectance of rough particulate media: ray-tracing solution. J Quant Spectrosc Radiat Transfer 2009;110(14–16):1418–40.
[31] Painter TH, Dozier J. Measurements of the hemispherical-directional reflectance of snow at fine spectral and angular resolution. J Geophys Res 2004;109:D18115. http://dx.doi.org/10.1029/2003JD004458.
[32] Painter T, Molotch N, Cassidy M, Flanner M, Steffen K. Contact spectroscopy for determination of stratigraphy of snow optical grain size. J Glaciol 2007;53:121–7.
[33] Picard G, Arnaud L, Domine F, Fily M. Determining snow specific surface area from near-infrared reflectance measurements: numerical study of the influence of grain shape. Cold Reg Sci Technol 2009;56(1):10–7.
[34] Sergent C, Leroux C, Pougatch E, Guirado F. Hemispherical-directional reflectance measurements of natural snow in the 0.9–1.45 μm spectral range: comparison with adding-doubling modeling. Ann Glaciol 1998;26:59–63.
[35] Shi Jiancheng, Davis RE, et al. Stereological determination of dry-snow parameters for discrete-scatterer microwave modeling. Ann Glaciol 1993;17:295–9.
[36] Stamnes K, Tsay S-C, Wiscombe WJ, Jayaweera K. Numerically stable algorithm for discrete-ordinate-method radiative transfer in multiple scattering and emitting layered media. Appl Opt 1988;27:2502–9.
[37] Thomas G, Stamnes K. Radiative transfer in the atmosphere and ocean.New York: Cambridge University Press; 517.
[38] Tsang L, Kong JA. Scattering of electromagnetic waves: advanced topics. Wiley-Interscience; 2001.
[39] Van de Hulst HC. Light scattering by small particles.New York: Dover Publications; 470.
[40] Warren Stephen G. Optical properties of snow. Rev Geophys 1982;20(1):67–89.
[41] Warren S. Optical constants of ice from the ultraviolet to the microwave. Appl Opt 1984;23:1206–25.
[42] Wiscombe Warren J, Warren Stephen G. A model for the spectral albedo of snow. I: pure snow. J Atmos Sci 1980;37(12):2712–33.
[43] Tanikawa T, Aoki T, Hori M, Hachikubo A, Aniya M. Snow bidirectional reflectance model using non-spherical snow particles and its validation with field measurements. EARSeL eProceedings 2006;5(2):137–45.
[44] Bohren Craig F, Beschta Robert L. Snowpack albedo and snow density, Cold Regions Science and Technology 1979;1(1):47–50, ISSN 0165-232X, http://dx.doi.org/10.1016/0165-232X(79)90018-1.